Output Feedback ILC for a Class of Nonminimum Phase Nonlinear Systems With Input Saturation: An Additive-State-Decomposition-Based Method

Zi-Bo Wei, Quan Quan, and Kai-Yuan Cai

***Abstract*—In this technical note, an additive-state-decomposition-based iterative learning control (ILC) method is proposed. Based on this method, the output feedback ILC problem is solved for a class of nonminimum phase (NMP) nonlinear systems with input saturation. This method is to "additively" decompose the output feedback ILC problem into two more tractable subproblems, namely an output feedback ILC problem for a linear time invariant (LTI) system and a state-feedback stabilization problem for a nonlinear system with input saturation. Then, a controller can be designed for each subproblem separately using existing methods, and the two designed controllers are combined together to achieve the original control goal. An illustrative example demonstrates the effectiveness of the proposed method.**

***Index Terms*—Additive state decomposition, iterative learning control, nonminimum phase nonlinear systems, saturation, tracking, uncertainties.**

I. Introduction

Iterative learning control (ILC) often applies to systems that repeat the same operation over a finite trial length $0 \leq t \leq T$. By using data recorded over previous trials and current-trial information, it aims to sequentially improve the performance of the operation as the trial index k increases [1]. System inversion plays a crucial role in the classical ILC design to approach perfect tracking [2]. However, for a nonminimum phase (NMP) system, the common system inversion is unstable. Thus, many special ILC designs for NMP systems were proposed. Stable inversion is a non-causal method to solve the tracking problem for NMP systems [3], [4] by avoiding the influence of the unstable zeros of the systems. However, completely accurate information about the systems is required. Therefore, if there exists any uncertainty about the systems, then the conventional stable inversion method cannot be used directly [5]. Based on the stable inversion, an adjoint-type ILC is proposed [6]–[12], which employs the adjoint operator to make the input to approach the stable inversion [5]. Because of online iterative process, the controller can deal with uncertainties, and obtain a better tracking result than that obtained by the conventional stable inversion method.

Manuscript received October 15, 2015; accepted April 12, 2016. Date of publication April 15, 2016; date of current version December 26, 2016. This work was supported by the National Natural Science Foundation of China under Grant 61473012. Recommended by Associate Editor L. Zaccarian.

Z-B. Wei was with the School of Automation Science and Electrical Engineering, Beihang University, Beijing 100191, China; and is now with the Shanghai Aircraft Design and Research Institute, Commercial Aircraft Corporation of China Ltd., Shanghai 201210, China (e-mail: whisper@buaa.edu.cn; weizibo@comac.cc).

Q. Quan and K-Y. Cai are with the School of Automation Science and Electrical Engineering, Beihang University, Beijing 100191, China (e-mail: qq_buaa@buaa.edu.cn; kycai@buaa.edu.cn).

Color versions of one or more of the figures in this paper are available online at http://ieeexplore.ieee.org.

Digital Object Identifier 10.1109/TAC.2016.2555081

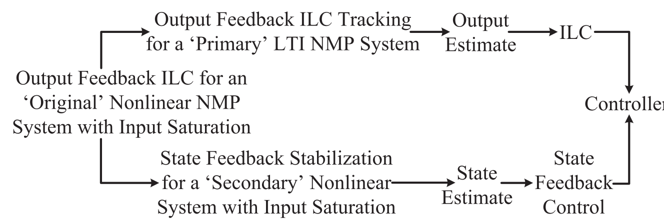

Fig. 1. The framework of the controller designed in this technical note.

As mentioned above, for a linear NMP system, there are many excellent results for the ILC tracking problem. However, for a nonlinear NMP system with input saturation, the research is relatively rare and there also exist three problems as follows:

i) It is somewhat complex to calculate the stable inversion. Moreover, all eigenvalues of $\boldsymbol{A}$ in the considered linearized systems (the form of it is the same as system (4)) are required to be real [3], [4], [8].
ii) Linearization or partial linearization is often used to transfer a nonlinear ILC problem to a linear ILC problem [11], [13]. The nonlinearity is ignored to some degree. This will decrease the convergence rate.
iii) The adjoint-type ILC requires a complicated modification to fit the input saturation [9], because it is a non-smooth and non-affine-in-input factor, like input deadzone mentioned in [14].

On the whole, the main difficulty of solving the output feedback ILC problem for a nonlinear NMP system with input saturation is caused by the tight coupling of input saturation, nonlinearity and the property of NMP. To deal with it, a method, called additive-state-decomposition-based (ASDB) ILC, is proposed. As shown in Fig. 1, it employs the additive state decomposition (ASD) [15], [16] to decompose the nonlinear NMP system into two subsystems, where the ILC control only needs to deal with an NMP linear time invariant (LTI) system separated from nonlinearity and input saturation. Concretely, NMP is assigned to a linear system for an output feedback ILC task, while the input saturation and nonlinearity are assigned to a nonlinear system for a state feedback stabilization task. As a result, the subproblems for the decomposed subsystems are much easier.

The contributions of this note are as follows: i) the ASDB ILC method is proposed to solve the tracking problem for a class of nonlinear NMP systems with input saturation, and the convergence rate is higher than that of the method based on linearization; ii) the form of the controller is simple and design process is concise and effective; iii) more importantly, a bridge is built between the existing ILC methods for LTI systems and a class of nonlinear systems so that more ILC problems of nonlinear systems become tractable.

The following definitions are used in this note: $\|\boldsymbol{\alpha}\|_{[t_1,t_2]} = \sup_{t\in[t_1,t_2]} \|\boldsymbol{\alpha}(t)\|_2$, where $\boldsymbol{\alpha}$ is a function vector defined on $[t_1, t_2]$;

$\|\boldsymbol{\alpha}\|_{\mathcal{L}_2} = \sqrt{\int_0^T \boldsymbol{\alpha}^T(t)\boldsymbol{\alpha}(t)dt}$, where $\boldsymbol{\alpha}$ is a function vector defined on $[0,T]$; $\langle \boldsymbol{\alpha}_1, \boldsymbol{\alpha}_2 \rangle_{\mathcal{L}_2} = \int_0^T \boldsymbol{\alpha}_1^T(t)\boldsymbol{\alpha}_2(t)dt$, where $\boldsymbol{\alpha}_1, \boldsymbol{\alpha}_2$ is a function vector defined on $[0,T]$; $\|\boldsymbol{\alpha}\|_2 = \sqrt{\boldsymbol{\alpha}^T\boldsymbol{\alpha}}$, where $\boldsymbol{\alpha}$ is a vector; $\|\mathcal{G}\| = \sup_{\|x\|_{\mathcal{L}_2}\le 1} \|\mathcal{G}x\|_{\mathcal{L}_2}$, where x is a function defined on $[0,T]$; $\mathcal{G}^*$ is the adjoint operator of $\mathcal{G}$, defined by $\langle y, \mathcal{G}u\rangle = \langle \mathcal{G}^* y, u\rangle$.

II. Problem Formulation and Preliminary Result

A. Problem Formulation

Consider a class of NMP nonlinear systems with input saturation as follows:

$$\begin{cases} \dot{\boldsymbol{x}}(t) = \boldsymbol{A}\boldsymbol{x}(t) + \boldsymbol{b}\text{sat}\left[u(t)\right] + \boldsymbol{\phi}\left[y(t)\right] \\ y(t) = \boldsymbol{c}^T\boldsymbol{x}(t), \boldsymbol{x}(0) = 0 \end{cases} \tag{1}$$

where $\boldsymbol{x}(t) \in \mathbb{R}^n$ is the state vector, $y(t) \in \mathbb{R}$ is the output, $u(t) \in \mathbb{R}$ is the input, $\boldsymbol{A} \in \mathbb{R}^{n\times n}$ is a stable constant matrix (see *Remark 1*), $\boldsymbol{b}, \boldsymbol{c} \in \mathbb{R}^n$ are constant vectors, $\boldsymbol{\phi} : \mathbb{R} \to \mathbb{R}^n$ is a nonlinear function vector and the element of $\boldsymbol{\phi}$ satisfies the local Lipschitz condition on D, where $D \subset \mathbb{R}$ is an open connected set, the saturation function sat $[u(t)]$ is defined as follows:

$$\text{sat}\left[u(t)\right] = \begin{cases} u_{\min}, & u(t) < u_{\min} \\ u(t), & u_{\min} \le u(t) < u_{\max} \\ u_{\max}, & u_{\max} \le u(t). \end{cases} \tag{2}$$

It is assumed that only $y(t)$ is available from measurement, and the relative degree of the system is r. The reference trajectory $y_d \in \mathcal{L}_2[0,T]$ is known and sufficiently smooth, $t \ge 0$. In the following, for convenience, the variable t will be omitted except when necessary. Three assumptions are made on system (1).

Assumption 1: The pair $(\boldsymbol{A}, \boldsymbol{c})$ is observable.

Assumption 2: The reference trajectory y_d satisfies $d^r y_d/dt^r \in \mathcal{L}_\infty[0,T]$.

Assumption 3: There exists a u_d such that $u = u_d$ makes $y = y_d$, where $u_{\min} < u_d < u_{\max}$ on $[0,T]$.

Objective: Construct a sequence of control $u(t) = u_k(t)$ for system (1), $t \in [0,T]$ such that

$$\|y_d - y_k\|_{[0,T]} \to 0, \text{ as } k \to \infty \tag{3}$$

where y_k is the corresponding output driven by u_k, $k = 1, 2, \ldots$, and $u_1(t) = 0$, $t \in [0,T]$.

Remark 1: Under *Assumption 1*, the pair $(\boldsymbol{A}, \boldsymbol{c})$ is observable. Therefore, there always exists a vector $\boldsymbol{p} \in \mathbb{R}^n$ such that $\boldsymbol{A} + \boldsymbol{p}\boldsymbol{c}^T$ is stable. Consequently, system (1) can be formulated into $\dot{\boldsymbol{x}} = (\boldsymbol{A} + \boldsymbol{p}\boldsymbol{c}^T)\boldsymbol{x} + \boldsymbol{b}\text{sat}(u) + [\boldsymbol{\phi}(y) - \boldsymbol{p}y]$. Therefore, matrix $\boldsymbol{A}$ is assumed to be stable without loss of generality.

Remark 2: If $\boldsymbol{x}(0) = \boldsymbol{x}_0 \ne 0$, the methods mentioned in [6] or [17] can be employed to transform it to $\boldsymbol{x}(0) = 0$.

Remark 3: Since the proposed method in this note is an online iterative method, it can deal with the system uncertainties. The simulation results in Section IV-C show the details.

Remark 4: *Assumption 2* is a necessary condition of *Assumption 3* [3], [4]. Since y_d is a trajectory which can be designed, *Assumption 2* can be satisfied easily.

B. Preliminary Result

Consider the linear system as follows:

$$\begin{cases} \dot{\boldsymbol{x}} = \boldsymbol{A}\boldsymbol{x} + \boldsymbol{b}u \\ y = \boldsymbol{c}^T\boldsymbol{x}, \boldsymbol{x}(0) = 0 \end{cases} \tag{4}$$

where $\boldsymbol{A} \in \mathbb{R}^{n\times n}$ and $\boldsymbol{b}, \boldsymbol{c} \in \mathbb{R}^n$ are the same as those in system (1). Its corresponding linear operator is $\mathcal{G} : \mathcal{L}_2[0,T] \mapsto \mathcal{L}_2[0,T]$, defined as

$$\mathcal{G}u = \int_0^t \boldsymbol{c}^T e^{\boldsymbol{A}(t-\tau)}\boldsymbol{b}u(\tau)d\tau. \tag{5}$$

Define

$$a_k = \|\mathcal{G}^*\tilde{y}_k\|^2_{\mathcal{L}_2}, b_k = \|\tilde{y}_k\|^2_{\mathcal{L}_2}, c_k = \|\tilde{u}_k\|^2_{\mathcal{L}_2} \tag{6}$$

where $\tilde{y}_k = y_d - y_k, \tilde{u}_k = u_d - u_k$. For the linear system (4), a sequence of control input $\{u_k\}_{k=1}^\infty$ is constructed in *Lemma 1* such that $\|\tilde{y}_k\|_{[0,T]} \to 0$, as $k \to \infty$.

Lemma 1: For system (4), under *Assumptions 2–3*, suppose $u = u_k$, $k = 1, 2, \ldots$ where

$$u_{k+1} = u_k + \alpha_k \mathcal{G}^*\tilde{y}_k, u_1 = 0 \tag{7}$$

and $(b_k - \sqrt{b_k^2 - (1-\rho_k)a_k c_k})/a_k \le \alpha_k \le (b_k + \sqrt{b_k^2 - (1-\rho_k)a_k c_k})/a_k$ with $\rho_k \in [1 - (b_k^2/a_k c_k), 1)$. Then $\|\tilde{u}_k\|_{\mathcal{L}_2} \to 0$, $\|\tilde{y}_k\|_{\mathcal{L}_2} \to 0$, $\|\tilde{y}_k\|_{[0,T]} \to 0$, as $k \to \infty$. In particular, if $\rho_k = 1 - (b_k^2/a_k c_k)$, then $\alpha_k = b_k/a_k$, and then $\|\tilde{u}_k\|_{\mathcal{L}_2}$ converges fastest.

Proof: See Appendix A.

III. ASDB ILC Framework

By using the ASD [15], [16], the considered NMP nonlinear system (1) is decomposed into two systems: an NMP LTI system (8) including all external signals as the primary system, together with a nonlinear system (11) with input saturation as the secondary system. Since the output of the primary system and the states of the secondary system can be observed, the original ILC problem for system (1) is correspondingly decomposed into two subproblems: an output feedback ILC problem for an NMP LTI system and a state feedback stabilization problem. Thanks to the ASD, the ILC problem is independent of nonlinearity and input saturation. As a result, the two new subproblems are much easier than the original problem for the nonlinear NMP system with input saturation.

A. Additive State Decomposition

ASD is applied to system (1). The first "primary" system is chosen as

$$\text{Primary System}: \begin{cases} \dot{\boldsymbol{x}}_p = \boldsymbol{A}\boldsymbol{x}_p + \boldsymbol{b}u_p + \boldsymbol{\phi}(y_d) \\ y_p = \boldsymbol{c}^T\boldsymbol{x}_p, \boldsymbol{x}_p(0) = 0 \end{cases} \tag{8}$$

which is a single input single output linear system with a known external signal $\boldsymbol{\phi}(y_d)$. Then, by subtracting the primary system (8) from the original system (1), one has

$$\begin{cases} \dot{\boldsymbol{x}} - \dot{\boldsymbol{x}}_p = \boldsymbol{A}(\boldsymbol{x} - \boldsymbol{x}_p) + \boldsymbol{b}\left[\text{sat}(u) - u_p\right] \\ \qquad + \boldsymbol{\phi}(y) - \boldsymbol{\phi}(y_d) \\ y - y_p = \boldsymbol{c}^T(\boldsymbol{x} - \boldsymbol{x}_p), \boldsymbol{x}(0) - \boldsymbol{x}_p(0) = 0. \end{cases} \tag{9}$$

Then, by defining

$$\boldsymbol{x}_s = \boldsymbol{x} - \boldsymbol{x}_p, y_s = y - y_p \tag{10}$$

system (9) becomes

$$\text{Secondary System}: \begin{cases} \dot{\boldsymbol{x}}_s = \boldsymbol{A}\boldsymbol{x}_s + \boldsymbol{b}\left[\text{sat}(u_p + u_s) - u_p\right] \\ \qquad + \boldsymbol{\phi}(y_p + y_s) - \boldsymbol{\phi}(y_d) \\ y_s = \boldsymbol{c}^T\boldsymbol{x}_s(t), \boldsymbol{x}_s(0) = 0 \end{cases} \tag{11}$$

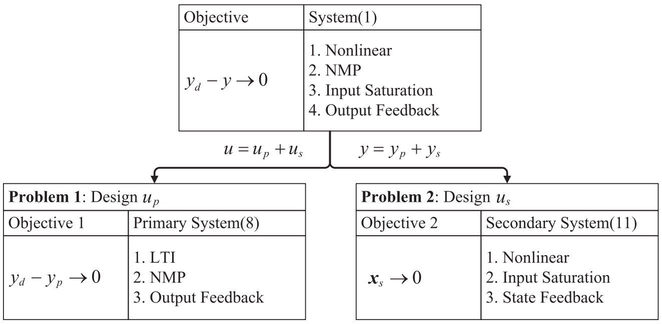

Fig. 2. Additive state decomposition for system (1).

which is a nonlinear system, where $u_s = u - u_p$. This is called the secondary system. According to (10), the state and the output satisfy

$$\boldsymbol{x} = \boldsymbol{x}_p + \boldsymbol{x}_s, y = y_p + y_s \tag{12}$$

where y_p and $\boldsymbol{x}_s$ are estimated by an observer stated in *Theorem 1*. Readers are suggested to refer to [15], [16] for details of ASD.

Theorem 1: Suppose that an observer is designed to estimate y_p and x_s in (8) and (11) as follows:

$$\begin{cases} \dot{\hat{\boldsymbol{x}}}_s = \boldsymbol{A}\hat{\boldsymbol{x}}_s + \boldsymbol{b}\,[\text{sat}(u) - u_p] + \boldsymbol{\phi}(y) - \boldsymbol{\phi}(y_d) \\ \hat{y}_p = y - \boldsymbol{c}^T\hat{\boldsymbol{x}}_s, \hat{\boldsymbol{x}}_s(0) = 0. \end{cases} \tag{13}$$

Then $\hat{y}_p \equiv y_p$ and $\hat{\boldsymbol{x}}_s \equiv \boldsymbol{x}_s$.

Proof: Subtracting (13) from (11) results in $\dot{\tilde{\boldsymbol{x}}}_s = \boldsymbol{A}\tilde{\boldsymbol{x}}_s$, $\tilde{\boldsymbol{x}}_s(0) = 0$, where $\tilde{\boldsymbol{x}}_s = \boldsymbol{x}_s - \hat{\boldsymbol{x}}_s$. Then, this implies that $\tilde{\boldsymbol{x}}_s \equiv 0$. Consequently, $\hat{y}_p \equiv y - \boldsymbol{c}^T\hat{\boldsymbol{x}}_s \equiv y_p$. □

Remark 5: If $y_d - y_p \equiv 0$, then $(\boldsymbol{x}_s, u_s) = 0$ is an equilibrium point of system (11). It is clear that if the controller $u_p = u_{p,k}$ drives $y_{p,k} \to y_d$ and the controller u_s drives $y_{s,k} \to 0$ as $k \to \infty$, then $y_k \to y_d$, as $k \to \infty$. The strategy here is to assign the ILC task to the primary system (8) and the stabilization task to the secondary system (11), respectively. According to these, the ASD offers a way to simplify the original control problem.

Remark 6: Since the primary system and the secondary system are virtual, so the initial value of the states can be assigned exactly for one of the systems. So, if $\boldsymbol{x}(0) = \boldsymbol{x}_0$ is uncertain in practice, still assign $\boldsymbol{x}_s(0) = 0$, leaving $\boldsymbol{x}_p(0) = \boldsymbol{x}_0$.

B. Two Problems

So far, the considered system is decomposed into two systems in charge of corresponding tasks. In this subsection, controller design in the form of problems is proposed with respect to the two component tasks, respectively. The whole process is shown in Fig. 2.

Problem 1 (on Primary System): For system (8), design an ILC input sequence

$$u_{p,k+1} = u_{p,k} + \mathcal{H}\tilde{y}_{p,k} \tag{14}$$

such that $\|\tilde{y}_{p,k}\|_{[0,T]} \to 0, \|\tilde{y}_{p,k}\|_{\mathcal{L}_2} \to 0, \|\tilde{u}_{p,k}\|_{\mathcal{L}_2} \to 0$ as $k \to \infty$, where $\tilde{y}_{p,k} = y_d - y_{p,k}, \tilde{u}_{p,k} = u_d - u_{p,k}$ and $\mathcal{H} : \mathcal{L}_2[0,T] \mapsto \mathcal{L}_2[0,T]$ is a linear operator.

Problem 2 (on Secondary System): For system (11), design a controller

$$u_{s,k} = \boldsymbol{l}^T\boldsymbol{x}_{s,k} \tag{15}$$

satisfies that $\|\boldsymbol{x}_{s,k}\|_{[0,T]} \to 0$, if $\|\tilde{y}_{p,k}\|_{\mathcal{L}_2} \to 0, \|\tilde{u}_{p,k}\|_{\mathcal{L}_2} \to 0$, where $\boldsymbol{l} \in \mathbb{R}^n$ is a constant vector.

With the two problems being solved, a theorem is obtained.

Theorem 2: For system (1), suppose i) *Problems 1–2* are solved and ii) the controller is designed as

$$\text{Observer}: \begin{cases} \dot{\hat{\boldsymbol{x}}}_{s,k} = \boldsymbol{A}\hat{\boldsymbol{x}}_{s,k} + \boldsymbol{b}\,[\text{sat}(u_k) - u_{p,k}] \\ \qquad + \boldsymbol{\phi}(y_k) - \boldsymbol{\phi}(y_d) \\ \hat{y}_{p,k} = y_k - \boldsymbol{c}^T\hat{\boldsymbol{x}}_{s,k}, \hat{\boldsymbol{x}}_{s,k}(0) = 0 \end{cases}$$
$$\text{Controller}: \begin{cases} u_{k+1} = u_{p,k} + \mathcal{H}\tilde{y}_{p,k} + \boldsymbol{l}^T\hat{\boldsymbol{x}}_{s,k+1} \\ u_1 = 0 \end{cases} \tag{16}$$

where $\tilde{y}_{p,k} = y_d - \hat{y}_{p,k}$. Then, the output of system (1) satisfies $\|\tilde{y}_k\|_{[0,T]} \to 0$, as $k \to \infty$.

Proof: Under condition i), it is easy to prove that if $k \to \infty$, then $\|\tilde{y}_k\|_{[0,T]} \leq \|\tilde{y}_{p,k}\|_{[0,T]} + \|y_{s,k}\|_{[0,T]} \to 0$ by using $\varepsilon - \delta$ definition. According to *Theorem 1*, the observer (13) will make $\hat{y}_p \equiv y_p$ and $\hat{x}_s \equiv x_s$. Then the controller (16) guarantees $\|\tilde{y}_k\|_{[0,T]} \to 0$, as $k \to \infty$. □

C. Solutions to Problems 1–2

1) Solution to Problem 1: The primary system (8) is expressed as

$$y_{p,k} = \mathcal{G}u_{p,k} + \mathcal{G}_d\,[\boldsymbol{\phi}(y_d)] \tag{17}$$

where $\mathcal{G}_d\boldsymbol{z} \triangleq \int_0^t \boldsymbol{c}^T e^{\boldsymbol{A}(t-\tau)}\boldsymbol{z}(\tau)d\tau$ and $\mathcal{G}$ is defined as (5). According to *Lemma 1*, a theorem is given, where the controller for the primary system can be designed by (18).

Theorem 3: For system (8), under *Assumptions 2–3*, suppose $u_p = u_{p,k+1}, k = 1, 2, \ldots$, where

$$u_{p,k+1} = u_{p,k} + \alpha_k\mathcal{G}^*\tilde{y}_{p,k}, u_{p,1} = 0 \tag{18}$$

and $(b_k - \sqrt{b_k^2 - (1-\rho_k)a_kc_k})/a_k \leq \alpha_k \leq (b_k + \sqrt{b_k^2 - (1-\rho_k)a_kc_k})/a_k$ with $\rho_k \in [1 - (b_k^2/a_kc_k), 1)$. By substituting $\tilde{y}_{p,k}, \tilde{u}_{p,k}$ for $\tilde{y}_k, \tilde{u}_k$, the definition of a_k, b_k, c_k is the same as in (6). Then $\|\tilde{u}_{p,k}\|_{\mathcal{L}_2} \to 0$, $\|\tilde{y}_{p,k}\|_{\mathcal{L}_2} \to 0$, $\|\tilde{y}_{p,k}\|_{[0,T]} \to 0$, as $k \to \infty$. In particular, if $\rho_k = 1 - (b_k^2/a_kc_k)$, then $\alpha_k = b_k/a_k$, and then $\|\tilde{u}_{p,k}\|$ converges fastest.

Proof: See Appendix C.

2) Solution to Problem 2: In fact, if *Problem 1* is well solved, then *Problem 2* will be solved indirectly by *Theorem 4*.

Theorem 4: For system (11), suppose that the controller u_s is designed as (15). Then, $\|\boldsymbol{x}_{s,k}\|_{[0,T]} \to 0$ as $\|\tilde{y}_{p,k}\|_{\mathcal{L}_2} \to 0$ and $\|\tilde{u}_{p,k}\|_{\mathcal{L}_2} \to 0$.

Proof: See Appendix D.

From the proof of *Theorem 4*, *Problem 2* can be theoretically solved by controller (15) with any $\boldsymbol{l}$ if $\|\tilde{y}_{p,k}\|_{\mathcal{L}_2} \to 0, \|\tilde{u}_{p,k}\|_{\mathcal{L}_2} \to 0$, as $k \to \infty$. However, the convergence rate may be unreasonable if $\boldsymbol{l}$ is inappropriate. For such a purpose, an index M in the following is proposed to choose $\boldsymbol{l}$. Linearizing system (11) along the nominal trajectory $(\boldsymbol{x}_{s,k}, y_{p,k}) = (0, y_d)$ results in

$$\dot{\boldsymbol{x}}_{s,k} = \underbrace{\left(\boldsymbol{A} + \boldsymbol{b}\boldsymbol{l}^T + \left.\frac{\partial\boldsymbol{\phi}(y_{p,k} + \boldsymbol{c}^T\boldsymbol{x}_{s,k})}{\partial\boldsymbol{x}_{s,k}}\right|_{\substack{y_{p,k}=y_d \\ \boldsymbol{x}_{s,k}=0}}\right)}_{\boldsymbol{A}_s(t)}\boldsymbol{x}_{s,k}$$
$$- \underbrace{\left.\frac{\partial\boldsymbol{\phi}\left(y_{p,k} + \boldsymbol{c}^T\boldsymbol{x}_{s,k}\right)}{\partial y_p}\right|_{\substack{y_{p,k}=y_d \\ \boldsymbol{x}_{s,k}=0}}}_{\boldsymbol{b}_s(t)}\tilde{y}_{p,k} + o(\tilde{y}_{p,k}, \boldsymbol{x}_{s,k}) \tag{19}$$

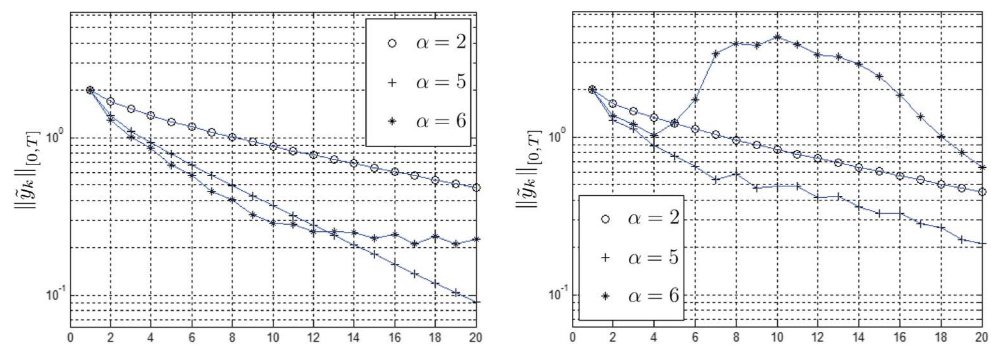

(a) $\delta_A = 0, \delta_\phi = 0$ (b) $\delta_A = -0.1, \delta_\phi = 0$

Fig. 3. The simulation results for ILC controller (29): (a) Convergence of $\|\tilde{y}_k\|_{[0,T]}$ when there is no uncertainty in the system; (b) Convergence of $\|\tilde{y}_k\|_{[0,T]}$ when there is an uncertainty in $\boldsymbol{A}$, that means $\boldsymbol{A}$ is replaced by $\boldsymbol{A}'$ for the original system (1).

where $o(\cdot)$ is the infinitesimal of higher order. Omitting $o(\cdot)$ leads to

$$\boldsymbol{x}_{s,k}(t) \approx -\int_0^t e^{\int_\tau^t \boldsymbol{A}_s(\alpha)d\alpha}\boldsymbol{b}_s(\tau)\tilde{y}_{p,k}(\tau)d\tau. \tag{20}$$

Then

$$\|\boldsymbol{x}_{s,k}\|_{[0,T]} \le M\|\tilde{y}_{p,k}\|_{[0,T]} \tag{21}$$

where

$$M = \int_0^T \left\| e^{\int_\tau^T \boldsymbol{A}_s(\alpha)d\alpha}\boldsymbol{b}_s(\tau)\right\|_2 d\tau. \tag{22}$$

Obviously, the index M determines the convergence rate, because the smaller M is, the higher the convergence rate will be. Roughly speaking, the chosen $\boldsymbol{l}$ should make $\dot{\boldsymbol{x}}_{s,k} = \boldsymbol{A}_s(t)\boldsymbol{x}_{s,k}$ stable.

Remark 7: From (21), it follows:

$$\begin{aligned}\|\tilde{y}_k\|_{[0,T]} &\le \|\tilde{y}_{p,k}\|_{[0,T]} + \|y_{s,k}\|_{[0,T]}\\ &\le (1 + M\|\boldsymbol{c}\|_2)\,\|\tilde{y}_{p,k}\|_{[0,T]}\end{aligned} \tag{23}$$

where $\boldsymbol{c}$ is defined in system (1). The convergence rate of the original system (1) depends on that of the primary system (8). Then, according to *Theorem 3*, a controller for the primary system should be designed to obtain a reasonable convergence rate so that the original system also converges fast.

IV. Simulation Results

A. Problem Formulation

Consider the nonlinear NMP system (1) with the following parameters: $u_{\min} = -15$, $u_{\max} = 3$, and

$$\boldsymbol{A} = \begin{bmatrix} 0 & 1 & 0\\ 0 & 0 & 1\\ -4 & -6 & -4\end{bmatrix},\ \boldsymbol{b} = \begin{bmatrix}0\\0\\1\end{bmatrix}$$

$$\boldsymbol{c} = \begin{bmatrix}-1\\0\\1\end{bmatrix},\ \boldsymbol{\phi}(y) = \begin{bmatrix}1-\cos y\\ 0\\ \sin y\end{bmatrix}. \tag{24}$$

It is obvious that *Assumption 1* holds. Since the zeros of the linear part are ± 1, the considered system is an NMP system. The objective is to design u to make $y \to y_d$ on $t \in [0, T]$ and $T = 6\pi$ in this example, where

$$y_d(t) = \begin{cases} 0, & 0 \le t < 2\pi\\ 1-\cos t, & 2\pi \le t < 4\pi\\ 0, & 4\pi \le t \le 6\pi.\end{cases} \tag{25}$$

In the following parts, some uncertainties are also considered. For instance

$$\boldsymbol{A}' = (1+\delta_A)\boldsymbol{A} \text{ and } \boldsymbol{\phi}' = (1+\delta_\phi)\boldsymbol{\phi} \tag{26}$$

where $\delta_A, \delta_\phi \in (-1, 1)$.

B. An Existing Method for Comparison

Although the classical ILC controller can deal with the NMP systems in theory, its convergence process is extremely slow and unacceptable [18]. Therefore, a comparable method is used for comparison. Because the ILC controller for the primary system is similar to the controller designed in reference [11], the controller in reference [11] is employed for comparison. First, by linearizing system (24) at $\boldsymbol{x} = 0$, one has

$$\begin{cases}\dot{\boldsymbol{x}} = \boldsymbol{A}_l\boldsymbol{x} + \boldsymbol{b}u\\ y = \boldsymbol{c}^T\boldsymbol{x}, \boldsymbol{x}(0) = 0\end{cases} \tag{27}$$

where

$$\boldsymbol{A}_l = \begin{bmatrix} 0 & 1 & 0\\ 0 & 0 & 1\\ -5 & -6 & -3\end{bmatrix} \tag{28}$$

and the corresponding operator of this system is denoted as $\mathcal{G}_l$. Then, the ILC controller is

$$u_{k+1} = u_k + \alpha\mathcal{G}_l^*\tilde{y}_k \tag{29}$$

where α is a constant which does not changed with k, and it is chosen as $\{2, 5, 6\}$ respectively. The adjoint operator $\mathcal{G}_l^* : \mathcal{L}_2[0,T] \mapsto \mathcal{L}_2[0,T]$ is calculated as follows [11], [12]:

$$\mathcal{G}_l^*\tilde{y} = \int_t^T \boldsymbol{b}^T e^{-\boldsymbol{A}_l^T(t-\tau)}\boldsymbol{c}\tilde{y}(\tau)d\tau. \tag{30}$$

Fig. 3 shows the simulation results.

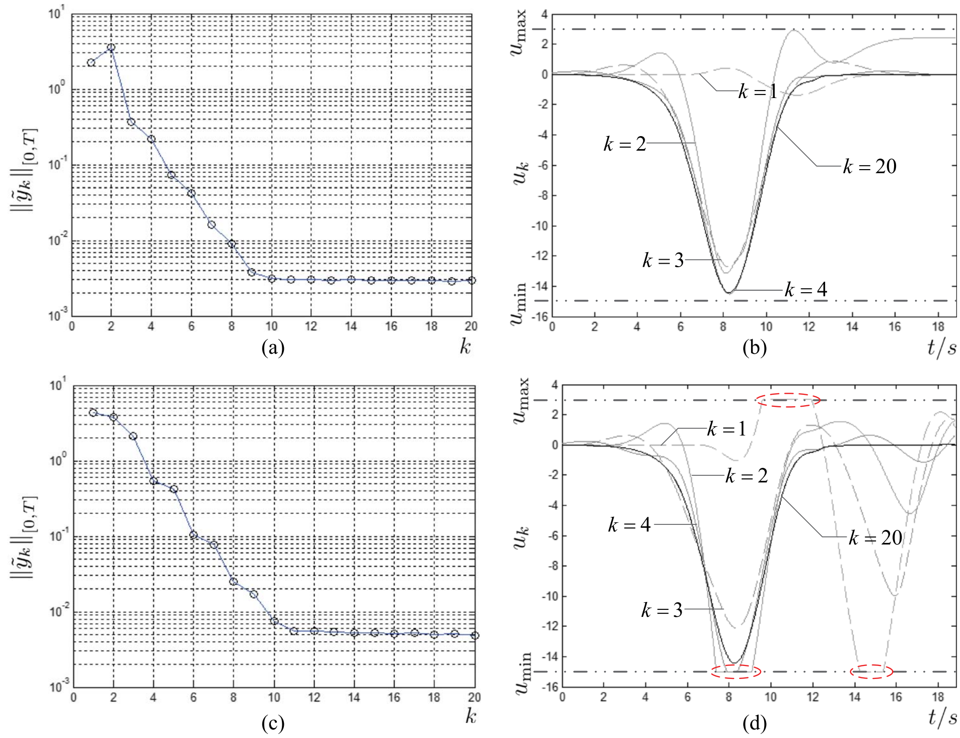

Fig. 4. The simulation results when the ASDB ILC controller (31) is adopted: (a), (b) Convergence of $\|\tilde{y}_k\|_{[0,T]}$ and the input serial $\{u_{1,k}\}_{k=1}^{20}$; (c)(d) Convergence of $\|\tilde{y}_k\|_{[0,T]}$ and the input serial $\{u_{2,k}\}_{k=1}^{20}$.

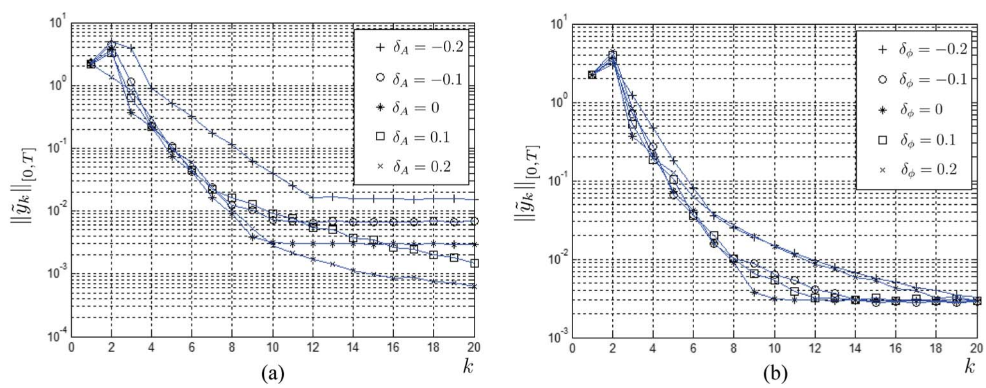

Fig. 5. The affect of the system uncertainty: (a) $\delta_A \in [-0.2, 0.2]$ and $\delta_\phi = 0$; (b) $\delta_\phi \in [-0.2, 0.2]$ and $\delta_A = 0$.

C. Controller Design and Simulation Result of ASDB ILC

1) Controller Design: For the controller (14), $u_{p,k+1} = u_{p,k} + \alpha_k \mathcal{G}^* \tilde{y}_{p,k}, \alpha_k = \|\tilde{y}_k\|^2_{\mathcal{L}_2} / \|\mathcal{G}^* \tilde{y}_k\|^2_{\mathcal{L}_2}$ is chosen, and the same method of calculating $\mathcal{G}_l^*$ is used to calculate $\mathcal{G}^*$. For the comparison purpose, $\boldsymbol{l}_1 = [-2\ -5\ -2]^T$ and $\boldsymbol{l}_2 = [1\ 5\ 1]^T$ are chosen for the controller (11). By (22), their indexes are calculated as $M_1 = 0.47$ and $M_2 = 10.49$. According to (16), the controller follows:

$$\begin{aligned} u_{i,k+1} &= u_{i,p,k+1} + u_{i,s,k+1} \\ &= u_{i,k} + \boldsymbol{l}_i^T (\hat{\boldsymbol{x}}_{i,s,k+1} - \hat{\boldsymbol{x}}_{i,s,k}) \\ &\quad + \alpha_k \mathcal{G}^* (y_d - \hat{y}_{i,p,k}),\ i = 1, 2. \end{aligned} \tag{31}$$

2) The Result by Controller (31): Driven by controller (31), the simulation results of $u_{i,k}$ are shown in Fig. 4(a)–(d), respectively, $i = 1, 2$. Based on these results, the following conclusions are derived: i) the reference trajectory is well-tracked from Fig. 4(a) and (c); ii) the input saturation does not affect the final tracking result from Fig. 4(d); iii) because $M_2 > M_1$, the convergence rate by $u_{2,k}$ is smaller than that by $u_{1,k}$ from Fig. 4(a) and (c), which is consistent with *Remark 7*; iv) the starting points of Fig. 4(a) and (c) are different, because $u_{2,k}$ generates a larger error in the secondary system; v) the convergence rate will be much higher than the existing method mentioned in Section IV-B.

3) The Affect of the System Uncertainty: In this part, δ_A, δ_ϕ are chosen from $[-0.2, 0.2]$. The controller is still chosen as shown in (31) (let $i = 1$), and $\boldsymbol{A}, \boldsymbol{\phi}$ are replaced with $\boldsymbol{A}', \boldsymbol{\phi}'$ for the original system (1). The simulation results are shown in Fig. 5, which illustrate that the controller proposed in this note is robust against these uncertainties. In this part, set $u_{\min} = -20$ to satisfy *Assumption 3* for all δ_A, δ_ϕ.

D. Discussions

From Fig. 3, the method mentioned in Section IV-B has two deficiencies: i) it is hard to choose a reasonable α_k to achieve a high convergence rate (the best performance is got at $\alpha = 5$, its convergence rate is still low); ii) when there are uncertainties in the system, the convergence rate is influenced remarkably. The reason of these phenomenons is that this kind of methods depends on linearization, and the convergence condition depends on the difference between the original system and the linearized system. The learning gain α must be small to adapt the difference. As a result, the convergence rate is low correspondingly. Reference [12] improves this method by using state feedback linearization. However, it uses not only the information of the output but also the informations of the states, which are not available in the output feedback control problem proposed in this note. Moreover, the convergence rate is not improved.

However, by ASD, the original system is separated into two parts instead of linearization. The primary system is an exact linear system with a known external signal $\phi(y_d)$, and all the necessary informations can be observed from the output of the original system by the observer (13). Then, the excellent linear conclusion (*Lemma 1* and *Theorem 3*) can be used to design the ILC controller to achieve a high convergence rate. In addition, the differences between the original system and the primary system are all contained in the secondary system. Then, a state feedback controller can be designed to eliminate these differences, even some strong nonlinear terms such as the saturation.

V. Conclusion

In this note, the output tracking problem for a class of nonlinear NMP systems with input saturation is solved by the ASDB ILC method. The main contribution of this note is that the complex controller design is avoided based on ASD instead of linearization. A bridge is built between the existing ILC design methods for LTI systems and a class of nonlinear systems so that more ILC problems of nonlinear systems become tractable. According to that, the existing adjoint-type ILC controller and the conventional state feedback controller are combined to solve the problem. The simulation results illustrate that: i) the structure of the proposed method is simple; ii) the convergence rate of it is high; iii) it is robust against the uncertainties of the original system.

Appendix

A. Proof of Lemma 1

This proof is organized as follows: (i) proves $\|\tilde{u}_k\|_{\mathcal{L}_2} \to \tilde{u}_\infty$ as $k \to \infty$ where $\tilde{u}_\infty$ is a constant; (ii) proves $\tilde{u}_\infty = 0$ by contradiction; (iii) $\|\tilde{y}_k\|_{\mathcal{L}_2} \to 0$ as $\|\tilde{u}_k\|_{\mathcal{L}_2} \to 0$, (iv) $\|\tilde{y}_k\|_{[0,T]} \to 0$ as $\|\tilde{u}_k\|_{\mathcal{L}_2} \to 0$.

(i) According to controller (7), one has

$$\tilde{u}_{k+1} = (I - \alpha_k \mathcal{G}^* \mathcal{G})\tilde{u}_k. \tag{32}$$

At step k, given a constant $\rho_k \in [0, 1)$ satisfying

$$\|\tilde{u}_{k+1}\|^2_{\mathcal{L}_2} \le \rho_k \|\tilde{u}_k\|^2_{\mathcal{L}_2} \tag{33}$$

one has

$$\|\tilde{u}_{k+1}\|^2_{\mathcal{L}_2} - \rho_k \|\tilde{u}_k\|^2_{\mathcal{L}_2} = a_k \alpha_k^2 - 2b_k \alpha_k + (1 - \rho_k)c_k \tag{34}$$

where a_k, b_k, c_k are defined in (6). Then

$$\alpha_{k\min} \le \alpha_k \le \alpha_{\max} \tag{35}$$

where $\alpha_{k\min} = (b_k - \sqrt{b_k^2 - (1-\rho_k)a_k c_k})/a_k$ and $\alpha_{\max} = (b_k + \sqrt{b_k^2 - (1-\rho_k)a_k c_k})/a_k$. This implies that

$$\rho_k \ge 1 - \frac{b_k^2}{a_k c_k} \tag{36}$$

must be satisfied. According to the property of inner product, $\|\tilde{y}_k\|^2_{\mathcal{L}_2} = \langle \tilde{y}_k, \mathcal{G}\tilde{u}_k \rangle_{\mathcal{L}_2} \le \|\mathcal{G}^* \tilde{y}_k\|_{\mathcal{L}_2} \|\tilde{u}_k\|_{\mathcal{L}_2}$, that means $0 \le b_k^2 / a_k c_k \le 1$ according to (6). Thus, $\{\|\tilde{u}_k\|_{\mathcal{L}_2}\}_{k=1}^{\infty}$ is bounded and decreases monotonically, namely $\|\tilde{u}_k\|_{\mathcal{L}_2} \to \tilde{u}_\infty$, as $k \to \infty$, where $\tilde{u}_\infty \ge 0$. Furthermore, choose $\rho_k = 1 - (b_k^2/a_k c_k)$, then $\alpha_k = b_k / a_k$ and $\|\tilde{u}_k\|_{\mathcal{L}_2}$ converges fastest.

(ii) Assuming $\tilde{u}_\infty > 0$, according to (33), one has

$$\tilde{u}_\infty^2 \le \rho_\infty^2 \tilde{u}_\infty^2. \tag{37}$$

According to (34)–(36), there exists a ρ_∞ that satisfies $\rho_\infty \ge 1 - b_\infty^2 / a_\infty c_\infty$ and (37). Since $\tilde{u}_\infty \ne 0$, $\tilde{y}_\infty = \mathcal{G}\tilde{u}_\infty \ne 0$, $b_\infty^2/a_\infty c_\infty = \varepsilon > 0$, one has $\tilde{u}_\infty^2 \le (1-\varepsilon)\tilde{u}_\infty^2$ by choosing $\rho = 1 - \varepsilon$. That means $\tilde{u}_\infty^2 < 0$, which is contradiction, therefore $\tilde{u}_\infty = 0$.

(iii) According to $\tilde{y}_k = \mathcal{G}\tilde{u}_k$, $\|\tilde{y}_k\|_{\mathcal{L}_2} \le \|\mathcal{G}\| \|\tilde{u}_k\|_{\mathcal{L}_2}$. Since system (4) is a linear system operating on a closed interval, $\|\mathcal{G}\|$ is bounded. Thus, $\|\tilde{y}_k\|_{\mathcal{L}_2} \to 0$ as $\|\tilde{u}_k\|_{\mathcal{L}_2} \to 0$.

(iv) According to (5), for $t \in [0, T]$

$$\begin{aligned} \|\tilde{y}_k(t)\|_2 &\le \sqrt{\int_0^t \|\boldsymbol{c}^T e^{\boldsymbol{A}(t-\tau)} \boldsymbol{b} \tilde{u}_k(\tau)\|_2^2 \, d\tau} \\ &\le \sqrt{\int_0^T \|\boldsymbol{c}^T e^{\boldsymbol{A}(t-\tau)} \boldsymbol{b}\|_2^2 \, d\tau} \|\tilde{u}_k\|_{\mathcal{L}_2}. \end{aligned} \tag{38}$$

Then

$$\begin{aligned} \|\tilde{y}_k\|_{[0,T]} &= \sup_{t\in[0,T]} \|\tilde{y}_k(t)\|_2 \\ &\le \left(\sup_{t\in[0,T]} \sqrt{\int_0^T \|\boldsymbol{c}^T e^{\boldsymbol{A}(t-\tau)} \boldsymbol{b}\|_2^2 \, d\tau} \right) \|\tilde{u}_k\|_{\mathcal{L}_2}. \end{aligned} \tag{39}$$

Since $\sup_{t\in[0,T]} \sqrt{\int_0^T \|\boldsymbol{c}^T e^{\boldsymbol{A}(t-\tau)} \boldsymbol{b}\|_2^2 d\tau}$ is bounded, $\|\tilde{y}_k\|_{[0,T]} \to 0$ as $\|\tilde{u}_k\|_{\mathcal{L}_2} \to 0$.

B. Proof of Theorem 3

According to (17), a new system is defined as

$$\bar{y}_{p,k} = \mathcal{G} u_{p,k} \tag{40}$$

where $\bar{y}_{p,k} = y_{p,k} - \mathcal{G}_d[\boldsymbol{\phi}(y_d)]$. Correspondingly, the reference trajectory becomes

$$\bar{y}_d = y_d - \mathcal{G}_d \left[\boldsymbol{\phi}(y_d)\right]. \tag{41}$$

Because $\mathcal{G}_d$ is a continuous linear operator and y_d satisfies *Assumption 2*, $\bar{y}_d$ also satisfies *Assumption 2*. The tracking error is $\tilde{\bar{y}}_{p,k} = \bar{y}_d - \bar{y}_{p,k} = y_d - (\mathcal{G} u_{p,k} + \mathcal{G}_d[\boldsymbol{\phi}(y_d)])$. Based on (17) and the definition of $\tilde{y}_{p,k}$, $\tilde{\bar{y}}_{p,k} = \tilde{y}_{p,k}$. Apply *Lemma 1* to system (40), if the controller is designed as shown in (18), then $\|\tilde{u}_{p,k}\|_{\mathcal{L}_2} \to 0$, $\|\tilde{y}_{p,k}\|_{\mathcal{L}_2} \to 0$, $\|\tilde{y}_{p,k}\|_{[0,T]} \to 0$, as $k \to \infty$. In particular, if $\rho_k = 1 - (b_k^2/a_k c_k)$, then $\alpha_k = b_k/a_k$ and $\|\tilde{u}_{p,k}\|_{\mathcal{L}_2}$ converges fastest.

C. Proof of Theorem 4

System (11) with the controller u_s designed as (15) is expressed as follows:

$$\dot{\boldsymbol{x}}_{s,k} = \boldsymbol{f}(t, \boldsymbol{x}_{s,k}, \boldsymbol{\lambda}_{p,k}), \boldsymbol{x}_{s,k}(0) = 0, \ t \in [0, T] \tag{42}$$

where $\boldsymbol{\lambda}_{p,k} = [\tilde{u}_{p,k}, \tilde{y}_{p,k}]^T$. Let $\boldsymbol{y}(t)$ and $\boldsymbol{z}(t)$ be solutions of

$$\dot{\boldsymbol{y}} = \boldsymbol{f}(t, \boldsymbol{y}, 0), \text{ and } \dot{\boldsymbol{z}} = \boldsymbol{f}(t, \boldsymbol{z}, \boldsymbol{\lambda}_{p,k}), \ t \in [0, T] \tag{43}$$

where $\boldsymbol{y}(0) = \boldsymbol{z}(0) = 0$. Then, for $t \in [0, T]$

$$\|\boldsymbol{y}(t) - \boldsymbol{z}(t)\|_2 \leq \int_0^t \|\boldsymbol{f}(\tau, \boldsymbol{y}(\tau), 0) - \boldsymbol{f}(\tau, \boldsymbol{z}(\tau), \boldsymbol{\lambda}_{p,k}(\tau))\|_2 \, d\tau. \tag{44}$$

Because $\boldsymbol{\phi}(\cdot)$ and $\mathrm{sat}(\cdot)$ satisfy the local Lipschitz condition, $\boldsymbol{f}$ also satisfies the local Lipschitz condition on $[0, T] \times D_1 \times D_2$, where $D_1 \subset \mathbb{R}^n$ and $D_2 \subset \mathbb{R}^2$ are open connected STEs, and that means

$$\|\boldsymbol{y}(t) - \boldsymbol{z}(t)\|_2 \leq \int_0^t \left(L_1 \|\boldsymbol{y}(\tau) - \boldsymbol{z}(\tau)\|_2 + L_2 \|\boldsymbol{\lambda}_{p,k}(\tau)\|_2\right) d\tau$$
$$\leq L_2 \|\boldsymbol{\lambda}_{p,k}\|_{\mathcal{L}_2} + L_1 \int_0^t \|\boldsymbol{y}(\tau) - \boldsymbol{z}(\tau)\|_2 \, d\tau \tag{45}$$

where L_1, L_2 are the corresponding Lipschitz constants. Applying the Gronwall-Bellman inequality to $\|\boldsymbol{y}(t) - \boldsymbol{z}(t)\|_2$ results in

$$\|\boldsymbol{y}(t) - \boldsymbol{z}(t)\|_{[0,T]} = \sup_{t \in [0,T]} \|\boldsymbol{y}(t) - \boldsymbol{z}(t)\|_2$$
$$\leq L_2 \|\boldsymbol{\lambda}_{p,k}\|_{\mathcal{L}_2} \sup_{t \in [0,T]} \left(1 + L_1 \int_0^t e^{L_1(t-\tau)} d\tau\right). \tag{46}$$

It is obvious that: (i) $\sup_{t \in [0,T]}(1 + L_1 \int_0^t e^{L_1(t-\tau)} d\tau)$ is bounded on $[0, T]$; (ii) according to system (11) and (15), $\boldsymbol{y}(t) = 0$; (iii) $\|\tilde{u}_{p,k}\|_{\mathcal{L}_2} \to 0$, $\|\tilde{y}_{p,k}\|_{\mathcal{L}_2} \to 0$ results in $\|\boldsymbol{\lambda}_{p,k}\|_{\mathcal{L}_2} \to 0$. Thus, $\|\boldsymbol{x}_{s,k}\|_{[0,T]} \to 0$ as $\|\tilde{u}_{p,k}\|_{\mathcal{L}_2} \to 0$, $\|\tilde{y}_{p,k}\|_{\mathcal{L}_2} \to 0$.

References

[1] D. H. Owens, C. T. Freeman, and T. Dinh Van, "Norm optimal iterative learning control with intermediate point weighting: Theory, algorithms and experimental evaluation," *IEEE Trans. Control Syst. Technol.*, vol. 21, no. 3, pp. 999–1007, 2013.

[2] T. Sogo, "On the equivalence between stable inversion for nonminimum phase systems and reciprocal transfer functions defined by the two-sided Laplace transform," *Automatica*, vol. 46, pp. 122–126, 2010.

[3] S. Devasia, D. Chen, and B. Paden, "Nonlinear inversion-based output tracking," *IEEE Trans. Autom. Control*, vol. 41, no. 7, pp. 930–942, 1996.

[4] L. R. Hunt and G. Meyer, "Stable inversion for nonlinear systems," *Automatica*, vol. 33, no. 8, pp. 1549–1554, 1997.

[5] K. Kinosita, T. Sogo, and N. Adachi, "Iterative learning control using adjoint systems and stable inversion," *Asian J. Control*, vol. 4, no. 1, pp. 60–67, 2002.

[6] N. Amann, D. H. Owens, and E. Rogers, "Iterative learning control for discrete-time systems with exponential rate of convergence," *Proc. Inst. Elect. Eng.*, vol. 143, no. 2, pp. 217–224, 1996.

[7] N. Amann, D. H. Owens, and E. Rogers, "lterative learning control using optimal feedback and feedforward actions," *Int. J. Control*, vol. 65, no. 2, pp. 277–293, 1996.

[8] J. Ghosh and B. Paden, "A pseudoinverse-based iterative learning control," *IEEE Trans. Autom. Control*, vol. 47, no. 5, pp. 831–837, 2002.

[9] B. Chu and D. H. Owens, "Iterative learning control for constrained linear systems," *Int. J. Control*, vol. 83, no. 7, pp. 1397–1413, 2010.

[10] S. Liu and T. J. Wu, "Robust iterative learning control design based on gradient method," in *Proc. 7th IFAC Symp. Adv. Control Chem. Processes*, 2004, pp. 687–692.

[11] T. Sogo, K. Kinoshita, and N. Adachi, "Iterative learning control using adjoint systems for nonlinear non-minimum phase systems," in *Proc. 39th IEEE Conf. Decision Control*, 2000, pp. 3445–3446.

[12] R. Ogoshi, T. Sogo, and N. Adachi, "Adjoint-type Iterative Learning Control for Nonlinear Nonminimum Phase System," in *Proc. 41st SICE Annu. Conf.*, 2002, pp. 1547–1550.

[13] G. M. Jeong and C. H. Choi, "Iterative learning control for linear discrete time nonminimum phase systems," *Automatica*, vol. 38, no. 2, pp. 287–291, 2002.

[14] J. X. Xu, J. Xu, and T. H. Lee, "Iterative learning control for systems with input deadzone," *IEEE Trans. Autom. Control*, vol. 50, no. 9, pp. 1455–1459, 2005.

[15] Q. Quan, K.-Y. Cai, and H. Lin, "Additive-state-decomposition-based tracking control framework for a class of nonminimum phase systems with measurable nonlinearities and unknown disturbances," *Int. J. Robust Nonlin. Control*, vol. 25, pp. 163–178, 2015.

[16] Q. Quan and K.-Y. Cai, "Additive decomposition and its applications to internal-model-based tracking," in *Proc. Joint 48th IEEE Conf. Decision Control & 28th Chinese Control Conf.*, 2009, pp. 817–822.

[17] M. Sun and D. Wang, "Iterative learning control with initial rectifying action," *Automatica*, vol. 38, no. 7, pp. 1177–1182, 2002.

[18] N. Amann and D. H. Owens, "Non-minimum Phase Plants in Iterative Learning Control," in *Proc. 2nd Int. Conf. Intell. Syst. Eng.*, 1994, pp. 107–112.